

Exceptional Dielectric Phase Transitions in a Perovskite-Type Cage Compound**

Wen Zhang,* Ying Cai, Ren-Gen Xiong,* Hirofumi Yoshikawa, and Kunio Awaga

Progress in metal–organic framework (MOF) research has recently opened up new possibilities to realize hybrid materials with unique solid-state electric properties, such as ferroelectricity, piezoelectricity, and dielectricity.^[1–5] Compared with conventional pure inorganic/organic compounds, MOFs take advantage of structural tunability and multifunctionality to develop polarizable molecular materials with rich dielectric properties. Among them, switchable molecular dielectrics, which undergo transitions between high and low dielectric states, are promising materials with potential applications especially in data communication, signal processing, and sensing. However, reports of such MOFs have remained scarce owing to a lack of knowledge regarding control of the motions of the dipole moments in the crystal lattice.

From the microscopic point of view, the tunable dielectric permittivity closely relates to the positional freedom of molecular dipole moments. For instance, polar molecules in the liquid state show larger dielectric permittivities than in the solid state owing to the “melting” and “freezing” of the molecular reorientations. With regard to MOFs, the dipole moments are rigidly fixed in the crystal structures in most cases, usually resulting in small and almost temperature-independent dielectric permittivities. Fortunately, there is still much room for the integration of flexible units into the frameworks; that is, the introduction of a polarization rotation unit in the form of a solid-state molecular rotator^[6–7] or host–guest systems, such as porous compounds.^[2]

Cage compounds, which are assembled by the inclusion of guest species into the well-matched host cages, is a very promising class of switchable molecular dielectrics. The reorientations of the polar guests in the carefully designed cage compounds may give rise to large dielectric permittivities, which are characterized by a multidimensional liquid-like state, and their freezing will lead to low-dielectric

systems. Herein, we present a novel organic–inorganic hybrid cage compound (HIm)₂[KFe(CN)₆] (**1**; HIm = imidazolium) with a perovskite-type structure, in which the order–disorder behavior of the HIm polar guests give rise to striking dielectric anomalies.

The (HIm)₂[KFe(CN)₆] crystals were grown from an aqueous solution of K₃[Fe(CN)₆] and (HIm)Cl salts by slow evaporation at room temperature as large red hexagonal plate perpendicular to the *c* axis. The existence of HIm and CN groups in **1** is verified by IR spectra. The CN group in **1** exhibits several vibrations in the range 2102–2143 cm^{−1}, distinct from a single peak of 2118 cm^{−1} in K₃[Fe(CN)₆]. Thermal analysis reveals that **1** undergoes two phase transitions, at 187 K (*T*₁) and 158 K (*T*₂). For convenience, we label the phase above *T*₁ as the high-temperature phase (HTP), the phase between *T*₁ and *T*₂ as intermediate-temperature phase (ITP), and the phase below *T*₂ as low-temperature phase (LTP).

Variable-temperature X-ray diffraction analysis reveals that **1** crystallizes in the centrosymmetric space group *R*3̄*m* at 293 K and 173 K as the HTP and ITP, respectively, and in *C*2/*c* at 83 K as the LTP.^[8] The common structural feature of the compound is the anionic cage formed by Fe–CN–K units in which the HIm cation resides. The metal–cyanide bond is strong and covalent in the fragment {Fe(CN)₆} (Fe–C = 1.9 Å) and much weaker and ionic in the fragment {K(NC)₆} (K–N = 2.9 Å; Figure 1). In the HTP, the cation reorients around the threefold *c* axis perpendicular to the ring plane. The cation consists of three carbon and two nitrogen atoms, which were all refined as carbon atoms. The five atoms of the

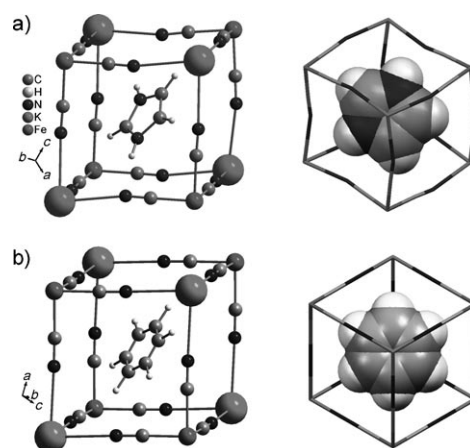


Figure 1. Crystal structures of **1** in the a) low-temperature (83 K) and b) high-temperature phase (293 K). Large corner spheres K, small corner spheres Fe; black N, gray C, small pale gray H.

[*] Prof. W. Zhang, Y. Cai, Prof. R.-G. Xiong
Ordered Matter Science Research Center, Southeast University
Nanjing 211189 (P. R. China)
Fax: (+86) 25-5209-0626
E-mail: zhangwen@seu.edu.cn
xionggrg@seu.edu.cn

Prof. H. Yoshikawa, Prof. K. Awaga
Research Center for Materials Science and
Department of Chemistry, Nagoya University
Furo-cho, Chikusa-ku, Nagoya 464-8602 (Japan)

[**] This work was supported by the National Natural Science Foundation of China (20951003, 20931002, and 90922005) and the NSF of Jiangsu Province (BK2008029).

Supporting information for this article is available on the WWW under <http://dx.doi.org/10.1002/ange.201001208>.

ring in the shape of pentagon are uniformly distributed over six apexes of a hexagon, as required by the crystal symmetry, revealing the existence of a highly dynamically disordered cation. Contrarily, the HIm cation in the LTP is totally frozen out to be ordered, and the carbon and the nitrogen atom are definitely distinguishable. The loss of the threefold symmetry results in the structure phase transition from a trigonal to a monoclinic system. There are eight HIm cations in the monoclinic unit cell, having four orientations with mutually cancelled dipole moments. As to the crystal structure at 173 K in the ITP, it adopts the same structure to that in the HTP, and little difference can be seen by comparing the crystal data parameters.

It is notable that **1** is one of a series of organic–inorganic hybrid cyano elpasolites $A_2[B'B''(CN)_6]$ (A = monovalent cation, $B' = K^I$ and its analogues, and $B'' = Cr^{III}, Mn^{III}, Fe^{III}, Co^{III}$).^[9] The cyano elpasolites can be considered as double perovskites with asymmetric CN ligand instead of the oxygen atom, and they are easily derived from the perovskite structure type by ordering the octahedrally coordinated B' and B'' cations over the B' sublattice in a chess-board manner. The cationic A guest resides in the large cage formed by $B'-NC-B''$. Considering the well-studied pure inorganic perovskite oxide materials (ABO_3), which exhibit many interesting and useful properties from both the theoretical and the applications point of view,^[10,11] the organic–inorganic hybrid materials with perovskite-type structures would afford a new type of electrically ordering solid-state systems by tuning the motions of polar A cations with external stimuli, such as temperature or electric field.

The temperature dependence of the real part of the complex relative dielectric permittivity (ϵ') of **1** was measured in three directions of the single-crystal sample. The crystal faces are selected in accordance with the structure in the HTP. Upon cooling, the dielectric permittivity along the $[1\bar{2}10]$ or $[10\bar{1}0]$ direction shows a gradual increase until it reaches a peak value of over 20 at T_1 (Figure 2 and Supporting Information). Then the permittivity exhibits a slight decrease followed by a plateau. At T_2 , it decreases sharply and then remains almost constant till 2 K at a value of approximately 6, which is characteristic of crystals with the “rotator phase” in HTP undergoing a freezing-out of the isotropic rotation of the polar HIm rings. A cooling/heating cycle shows a thermal hysteresis of about 4 K, thus revealing the nature of the first-order phase transition at T_2 . There is no dielectric relaxation

process in the close vicinity of the transition temperatures at different frequencies (see Supporting Information), indicating a relatively fast dipolar motion.^[12] The rotational dynamics of the HIm cation is currently under investigation on a similar compound $(HIm)_2[KCo(CN)_6]$ through a combination of solid-state NMR studies and molecular-mechanics calculations.

Another striking feature of the dielectric properties of **1** is the anisotropy; namely, the dielectric permittivities have a crystal-axis dependence. Large anomalies are observed in the HTP and ITP in the directions perpendicular to the threefold axis of the crystal lattice, while only a small anomaly is recorded in the whole temperature range in the direction of the threefold axis, thus confirming that the dielectric anisotropic properties are confined to the plane perpendicular to the threefold axis of the HTP. The dielectric anisotropy can be explained by examining the placement of the HIm cation in the $Fe-CN-K$ cage. It can be seen from the crystal structure that the cation lies in the plane perpendicular to the c axis in the HTP. Its in-plane rotation or disordering upon temperature changes never yields a dipole-moment component in the c axis, which leads to no change of the dielectric permittivity in this direction (the discernable small change originating from an imperfect c cut). The variation of permittivities in the plane perpendicular to the c axis is consistent with dielectric behaviors of some substances composed with polar molecules which exhibit free- and frozen-rotator phases. Furthermore, the variable-temperature dielectric permittivity under an applied magnet field of 5.0 Tesla was measured and no change occurs (see the Supporting Information). Taking into account the relatively small dielectric anomaly and the crystallographic data of **1** at various temperatures, it is clear that the phase transitions of **1** are neither ferroelectric nor antiferroelectric.^[13]

The two solid-state phase transitions of **1** were also revealed by calorimetric measurements. The molar heat capacity C_p of **1** was measured in the temperature range 100–220 K. One sharp heat capacity peak and a small discontinuous jump were observed at T_2 and T_1 , respectively, which corresponds well to the LTP-to-ITP and ITP-to-HTP transitions (Figure 3). From the C_p – T curve, an entropy change $\Delta S = 6.56 \text{ J mol}^{-1} \text{ K}^{-1}$ is obtained during the LTP-to-ITP transition. An estimation of the number of the molecular orientations from the calorimetric data can be made from the Boltzmann equation, $\Delta S = nR \ln(N)$, where n is the number of guest molecules per mole, R is the gas constant, and N is the

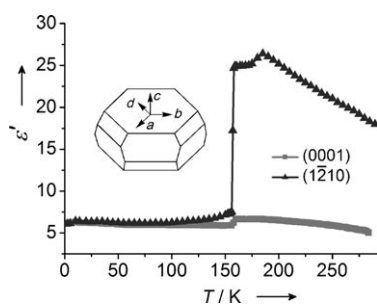


Figure 2. Anisotropic dielectric permittivities of the single crystal **1** measured at 1 MHz.

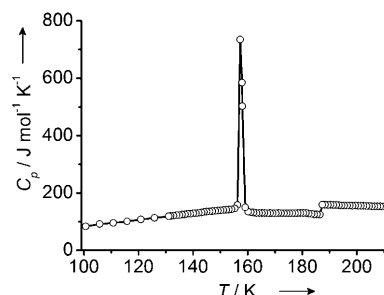


Figure 3. Temperature dependence of the molar heat capacity of **1**.

number of possible orientations for the disordered system. The calculated value of N per one HIm cation is 1.48, which reflects a more complex transition than a typical order–disorder transition undergoing reorientations at two sites ($N=2$). The small jump of C_p at T_1 reveals a more disordered structure of **1** in the HTP than the ITP. Although the variable-temperature X-ray single-crystal diffraction analysis discloses no observable structural changes in the HTP and ITP, the nature of this phase transition is not clear and needs further investigation. After all, the specific heat measurement reveals the similar dynamic disorder of the HIm cation in the HTP and ITP while it is completely frozen out in the LTP, as shown in the low-temperature crystallographic data. To further confirm the characteristics of the phase transitions, differential scanning calorimetry (DSC) measurement was taken, which definitely shows that a sharp peak appearing at around T_2 and a small peak at around T_1 (see the Supporting Information). With the above measurements, it is clear that the crystal of **1** undergoes a first-order phase transition at T_2 and a second-order transition at T_1 .

In conclusion, we have presented a new organic–inorganic hybrid cage compound **1** with the perovskite-type architecture. It exhibits two phase transitions at 158 K and 187 K. An order–disorder mechanism is found in the structural transformations owing to the motions of the cationic guests under different temperatures. Compound **1** represents a new class of switchable molecular dielectrics that shows striking dielectric anomalies and anisotropy. Investigations on such systems can shed light on the understanding of structural phase transitions of switchable molecular dielectrics and afford a useful strategy in searching for new electric ordering materials. A detailed study is now underway.

Experimental Section

All reagents and solvents in the syntheses were of reagent grade and were used without further purification. Evaporation of the aqueous solution (200 mL) of $K_3[Fe(CN)_6]$ (16.5 g, 0.05 mol) and (HIm)Cl (HIm = imidazolium; 15.0 g, 0.15 mol) results in the formation of **1** in the form of red crystals. IR (cm^{-1}): $\tilde{\nu}$ = 2102–2143 (vs, C≡N), 1467 (s, C=C), 1088 (vs, C–H).

X-ray diffraction experiments were carried out on **1** using a Rigaku CCD diffractometer with $\text{MoK}\alpha$ radiation ($\lambda = 0.71073 \text{ \AA}$) at various temperatures. Data collection, cell refinement and data reduction: CrystalClear 1.3.5 (Rigaku). The structure of **1** was solved by direct methods and refined by the full-matrix method based on F^2 using the SHELXL97 software package (Sheldrick, 1997). All non-hydrogen atoms were refined anisotropically and the positions of all hydrogen atoms were generated geometrically. CCDC 767143, CCDC 767144, and CCDC 767145 for **1** contains the supplementary crystallographic data for this paper. These data can be obtained free of charge from The Cambridge Crystallographic Data Centre via www.ccdc.cam.ac.uk/data_request/cif.

For dielectric measurements, the samples were made with single-crystals cut into the form of thin plates perpendicular to the crystal axes. Silver conduction paste deposited on the surfaces (surface ca. 10 mm^2) was used as the electrodes. Complex dielectric permittivity was measured with an Agilent 4294A impedance analyzer over the frequency range of from 2.5 kHz to 1 MHz with an applied electric

field of 0.5 V. Differential scanning calorimetry (DSC) measurements were performed on a PerkinElmer Diamond DSC. Specific heat analyses were carried out on a Quantum Design PPMS.

Received: February 27, 2010

Revised: May 11, 2010

Published online: August 16, 2010

Keywords: cage compounds · dielectrics · organic–inorganic hybrid composites · perovskite phases · phase transitions

- [1] S. Ohkoshi, H. Tokoro, T. Matsuda, H. Takahashi, H. Irie, K. Hashimoto, *Angew. Chem.* **2007**, *119*, 3302–3305; *Angew. Chem. Int. Ed.* **2007**, *46*, 3238–3241.
- [2] a) H.-B. Cui, K. Takahashi, Y. Okano, H. Kobayashi, Z.-M. Wang, A. Kobayashi, *Angew. Chem.* **2005**, *117*, 6666–6670; *Angew. Chem. Int. Ed.* **2005**, *44*, 6508–6512; b) H.-B. Cui, Z.-M. Wang, K. Takahashi, Y. Okano, H. Kobayashi, A. Kobayashi, *J. Am. Chem. Soc.* **2006**, *128*, 15074–15075; c) H.-B. Cui, B. Zhou, L.-S. Long, Y. Okano, H. Kobayashi, A. Kobayashi, *Angew. Chem.* **2008**, *120*, 3424–3428; *Angew. Chem. Int. Ed.* **2008**, *47*, 3376–3380.
- [3] a) P. Jain, N. S. Dalal, B. H. Toby, H. W. Kroto, A. K. Cheetham, *J. Am. Chem. Soc.* **2008**, *130*, 10450–10451; b) P. Jain, V. Ramachandran, R. J. Clark, H. D. Zhou, B. H. Toby, N. S. Dalal, H. W. Kroto, A. K. Cheetham, *J. Am. Chem. Soc.* **2009**, *131*, 13625–13627.
- [4] a) W. Zhang, R.-G. Xiong, S.-P. D. Huang, *J. Am. Chem. Soc.* **2008**, *130*, 10468–10469; b) W. Zhang, L.-Z. Chen, R.-G. Xiong, T. Nakamura, S.-P. D. Huang, *J. Am. Chem. Soc.* **2009**, *131*, 12544–12545; c) H.-Y. Ye, D.-W. Fu, Y. Zhang, W. Zhang, R.-G. Xiong, S. D. Huang, *J. Am. Chem. Soc.* **2009**, *131*, 42–43.
- [5] W. Zhang, H.-Y. Ye, R.-G. Xiong, *Coord. Chem. Rev.* **2009**, *253*, 2980–2997.
- [6] G. S. Kottas, L. I. Clarke, D. Horinek, J. Michl, *Chem. Rev.* **2005**, *105*, 1281–1376.
- [7] T. Akutagawa, H. Koshinaka, D. Sato, S. Takeda, S.-I. Noro, H. Takahashi, R. Kumai, Y. Tokura, T. Nakamura, *Nat. Mater.* **2009**, *8*, 342–347.
- [8] Crystal data for **1** at 293 K: $\text{C}_{12}\text{H}_{10}\text{FeKN}_{10}$, $M_r = 389.25$, trigonal, $R\bar{3}m$, $a = b = 8.7498(17) \text{ \AA}$, $c = 19.029(3) \text{ \AA}$, $\alpha = \beta = 90^\circ$, $\gamma = 120^\circ$, $V = 1261.7(4) \text{ \AA}^3$, $Z = 3$, $\rho_{\text{calcd}} = 1.537 \text{ g cm}^{-3}$, R_1 ($I > 2\sigma(I)$) = 0.0397, wR_2 (all data) = 0.1190, $m = 1.160 \text{ mm}^{-1}$, $S = 1.163$. **1** at 173 K: trigonal, $R\bar{3}m$, $a = b = 8.7632(11) \text{ \AA}$, $c = 18.8197(19) \text{ \AA}$, $\alpha = \beta = 90^\circ$, $\gamma = 120^\circ$, $V = 1251.6(3) \text{ \AA}^3$, $Z = 3$, $\rho_{\text{calcd}} = 1.549 \text{ g cm}^{-3}$, R_1 ($I > 2\sigma(I)$) = 0.1054, wR_2 (all data) = 0.2956, $m = 1.170 \text{ mm}^{-1}$, $S = 1.110$. **1** at 83 K: monoclinic, $C2/c$, $a = 13.462(12) \text{ \AA}$, $b = 8.767(7) \text{ \AA}$, $c = 15.125(14) \text{ \AA}$, $\beta = 111.93(4)^\circ$, $V = 1656(3) \text{ \AA}^3$, $Z = 4$, $\rho_{\text{calcd}} = 1.561 \text{ g cm}^{-3}$, R_1 ($I > 2\sigma(I)$) = 0.0636, wR_2 (all data) = 0.1181, $m = 1.179 \text{ mm}^{-1}$, $S = 1.146$.
- [9] a) B. I. Swanson, R. R. Ryan, *Inorg. Chem.* **1973**, *12*, 283–286; b) W. Massa, D. Babel, *Chem. Rev.* **1988**, *88*, 275–296.
- [10] L. G. Tejuca, J. L. G. Fierro, *Perovskites and Applications of Perovskite-type Oxides*, Marcel Dekker, New York, **1992**.
- [11] B. A. Strukov, A. P. Levanyuk, *Ferroelectric Phenomena in Crystals*, Springer, Berlin, **1998**.
- [12] a) R. Jakubas, A. Piecha, A. Pietraszko, G. Bator, *Phys. Rev. B* **2005**, *72*, 104107; b) B. Kulicka, V. Kinzhybalo, R. Jakubas, Z. Ciunik, J. Baran, W. Medycki, *J. Phys. Condens. Matter* **2006**, *18*, 5087–5104.
- [13] C. Kittel, *Phys. Rev.* **1951**, *82*, 729–732.